Korean J. Chem. Eng., **28**(3), 949-953 (2011)
DOI: 10.1007/s11814-010-0422-1

Effect of CO_2 concentration on the performance of different thermodynamic models for prediction of CH_4+CO_2+H_2O hydrate equilibrium conditions

Bahman Zarenezhad†, Mona Mottahedin, and Ali Haghighi Asl

School of Chemical, Petroleum and Gas Engineering, Semnan University, P. O. Box 35195-363, Semnan, Iran
(*Received 2 August 2010 • accepted 6 September 2010*)

Abstract−Accurate prediction of phase equilibria regarding CH_4 replacement in hydrate phase with high pressure CO_2 is an important issue in modern reservoir engineering. In this work we investigate the possibility of establishing a thermodynamic framework for predicting the hydrate equilibrium conditions for evaluation of CO_2 injection scenarios. Different combinations of equations of state and mixing rules are applied and the most accurate thermodynamic models at different CO_2 concentration ranges are proposed.

Key words: Gas Hydrate, Phase Equilibrium, CO_2 Injection, Methane Replacement, Reservoir

INTRODUCTION

Natural Gas hydrates are of particular interest in the petroleum industry as well as in the energy and environmental field. The most widely cited estimate of global hydrate-bound gas is about 21×10^{15} m^3 of methane at standard temperature and pressure conditions [1]. The amount of organic carbon contained in natural gas hydrate reserves is estimated to be twice the amount contained in all fossil fuels including coal, oil and conventional natural gas reserves [2]. This large gas hydrate reservoir is suggested as an important component of future energy resources.

Many researchers have studied recovering CH_4 hydrate from the ocean floor at various operating conditions [2]. Clathrate hydrates occur naturally in permafrost regions and in sub-sea sediment where existing pressures and temperatures allow for thermodynamic stability of the hydrate [3].

Replacement of CH_4 in the hydrate with high pressure CO_2 is a candidate for recovering CH_4 gas from its hydrates under the ocean [5,6]. This process is also a favorable way of long-term storage of CO_2 and enables the ocean floor to remain stabilized even after recovering the methane gas because the CH_4 hydrate has the same structure as the CO_2 hydrate of which the unit cell consists of six medium cages (M-cage) and two small cages (S-cage) [7]. Measurements of three phase equilibria (vapor-liquid-hydrate) for the ternary system show that the CO_2 hydrate is thermodynamically more stable than the CH_4 hydrate under low temperatures below 283 K, because the equilibrium pressure of the CO_2 hydrate is lower than that of the CH_4 hydrate. Hirohama et al. [8] conducted the replacement reaction with saturated liquid CO_2 at 274 K and implied that the driving force for the replacement is probably the fugacity difference between the fluid and the hydrate phases, assuming a direct replacement mechanism.

Since the prediction of phase equilibria regarding CH_4 replacement in hydrate with CO_2 is an important issue regarding methane gas exploitation and CO_2 sequestration, it is necessary to establish an accurate thermodynamic framework for predicting the hydrate equilibrium conditions for evaluation of CO_2 injection scenarios. Therefore, effect of CO_2 concentration on the performance of different thermodynamic models for prediction of CH_4+CO_2+H_2O hydrate equilibrium conditions has been investigated in this work.

†To whom correspondence should be addressed.
E-mail: zarenezhad@yahoo.com

THERMODYNAMIC MODEL

The difference of the chemical potential of water between the hydrate phase and the empty hydrate lattice can be derived from statistical thermodynamics [9]:

$$\Delta\mu_w^{H-MT}=\mu_w^H-\mu_w^{MT}=-\mathrm{RT}\sum_{m=1}^{NCA}\mathrm{v}_m\ln\left(1+\sum_{j=1}^{NH}\mathrm{C}_{mj}\hat{\mathrm{f}}_j^V\right) \tag{1}$$

where μ_w^H and μ_w^{MT} are the chemical potential of water in hydrate phase and in empty lattice, respectively; v_m the number of cavities of type m per water molecule in the hydrate phase; C_{mj} the Langmuir constant of component j on the cavity of type m, and $\hat{f}_j^V$ is the fugacity of component j in the vapor phase with which the hydrate phase is in equilibrium.

The difference of the chemical potential of water between the empty hydrate lattice and the liquid phase can be expressed by:

$$\Delta\mu_w^{MT-L}=\mu_w^{MT}-\mu_w^L=\Delta\mu_w^0-\mathrm{RT}\int_{T_0}^{T}\frac{\Delta\mathrm{h}_w^{MT-L}}{\mathrm{RT}^2}\mathrm{dT}+\mathrm{RT}\int_{P_0}^{P}\frac{\Delta\mathrm{v}_w^{MT-L}}{\mathrm{RT}}\mathrm{dP}-\mathrm{RT}\ln(\gamma_w\mathrm{x}_w) \tag{2}$$

where μ_w^L is the chemical potential of water in the liquid phase; $\Delta\mu_w^0$, Δh_w^{MT-L} and Δv_w^{MT-L} are the water chemical potential difference at the reference condition, the water enthalpy difference and the water molar volume difference between the empty hydrate lattice and the liquid phase, respectively. x_w and γ_w are the water mole fraction and its activity coefficient.

At thermodynamic equilibrium, the chemical potential of water in hydrate and liquid phases is equal such that the following equation is satisfied:

$$\mu_w^H=\mu_w^L \tag{3}$$

Since water concentration is much higher than that of other species in the liquid phase, x_w and γ_w in Eq. (2) are both very close to one. Therefore, the following equation can be derived by combining Eqs. (1)-(3):

$$\Delta\mu_w^0 - RT\int_{T_0}^{T}\frac{\Delta h_w^{MT-L}}{RT^2}dT + RT\int_{P_0}^{P}\frac{\Delta v_w^{MT-L}}{RT}dP - RT\sum_{m=1}^{NCA}v_m\ln\left(1+\sum_{j=1}^{NH}C_m\hat{f}_j^{V}\right)=0 \quad (4)$$

The Langmuir constant in Eq. (4) can be determined by using the Lennard-Jones-Devonshire cell theory [6]:

$$C_{mj}=\frac{4\pi}{kT}\int_0^{R_c}\exp\left[\frac{-w(r)}{kT}\right]r^2dr \quad (5)$$

where r is the radial distance from the cavity center, w(r) is the spherical-core potential and k is Boltzmann's constant. In the present study, the Kihara potential with spherical core is used for the cavity potential function because it has been reported to give better results than the Lennard-Jones potential. By summing over all guest-water interactions in the cavity, we obtain the spherical core potential as follows:

$$w(r)=2Z\varepsilon\left[\frac{\sigma^{12}}{R^{11}r}\left(\delta^{10}+\frac{a}{R}\delta^{11}\right)-\frac{\sigma^{6}}{R^{5}r}\left(\sigma^{4}+\frac{a}{R}\sigma^{5}\right)\right] \quad (6)$$

With

$$\sigma^N=\frac{1}{N}\left[\left(1-\frac{r}{R}-\frac{a_c}{R}\right)^{-N}-\left(1+\frac{r}{R}-\frac{a_c}{R}\right)^{-N}\right] \quad (7)$$

where R is the cell radius of the cavity, N is an exponent number, Z is the coordination number, a_c is the Kihara hard core parameter, ε is the characteristic energy and σ is Kihara size parameter.

The fugacities of all components in the vapor and liquid phases are determined by using a cubic equation of state (EOS). At equilibrium the calculated $\hat{f}_j^{V}$ values should satisfy Eq. (4). The general form of a cubic EOS is given by:

$$P=\frac{RT}{v-b}-\frac{a}{v^2+Uv+W} \quad (8)$$

Depending on the numerical values of U and W, various equations of state can be obtained.

Incorporation of U=1 and W=0 in Eq. (8) leads to the Soave-Redlich-Kwong (SRK) EOS [10] with the following two parameters:

$$a=0.42747R^2T_c^2\alpha(Tr)/P_c \quad (9)$$

$$b=0.08664RT_c/P_c \quad (10)$$

where

$$\alpha(T_r)=(1+m_s(1-T_r^{0.5})^2 \quad (11)$$

and

$$m_s=0.480+1.574\omega-0.176\omega^2 \quad (12)$$

For the case of U=b+c, W=−bc, the Valderrama-Patel-Teja (VPT) EOS [11] with the following parameters is derived:

$$a=(0.66121-0.76105Z_c)R^2T_c^2\alpha(T_r)/P_c \quad (13)$$

$$b=(0.02207+0.20868Z_c)RT_c/P_c \quad (14)$$

$$c=(0.57765-1.87080Z_c)RT_c/P_c \quad (15)$$

where

$$\alpha(T_r)=(1+F(1-T_r^{0.5})^2 \quad (16)$$

The subscripts c and r denote critical and reduced properties, respectively. The coefficient F is given by:

$$F=0.46286+3.58230(\omega Z_c)+8.19417(\omega Z_c)^2 \quad (17)$$

where Z_c is the critical compressibility factor, and ω is the acentric factor.

In this work the mixing rule suggested by Avlonitis et al. (ADT) [12] which takes the polar-nonpolar interactions into account is used and the results are compared with those obtained through conventional van der Waals (VW) mixing rule [10]. The mixing rules formulations are given below:

a) van der Waals (VW) mixing rule:

The parameters a and b can be expressed as:

$$a=\sum_{i=1}^{NC}\sum_{j=1}^{NC}x_ix_ja_{ij}(1-k_{ij}) \quad (18)$$

where $a_{ij}=(a_ia_j)^{0.5}$ and k_{ij} is the interaction coefficient such that $k_{ii}=0$ and k_{ji}.

$$b=\sum_{i=1}^{NC}x_ib_i \quad (19)$$

b) Avlonitis et al. (ADT) mixing rule:

According this mixing rule, the parameter a is modified as follows:

$$a=a^W+a^A \quad (20)$$

where a^W is given by Eq. (18) and the term a^A corrects for asymmetric interaction:

$$a^A=\sum_{P=1}^{NP}x_P^2\sum_{i=1}^{NC}x_ia_{Pi}l_{Pi} \quad (21)$$

where

$$a_{pi}=(a_pa_i)^{0.5} \quad (22)$$

where p is the index of polar component and l_{pi} is the binary interaction parameter between the polar component and the other species determined by the following equation [12]:

$$l_{Pi}=l_{Pi}^0-l_{Pi}^1(T-T_0) \quad (23)$$

l_{pi}^0 and l_{pi}^1 are binary interaction parameters such that $l_{ii}=0$ and $l_i=l_{ji}$ and T_0 is the freezing point of water in K. Eq. (19) is used for calculation of b parameter.

The equilibrium pressure of $CO_2+CH_4+H_2O$ hydrate at a given temperature can be calculated according to the following solution procedure:

1. T, z_i and physical properties are used as model input.
2. P, x_i and y_i are assumed.
3. Flash calculation using an EOS at T and P is carried out.
4. x_i, y_i, $\hat{f}_i^{L}$, $\hat{f}_i^{V}$ of all components are determined.
5. H-V-L_w equilibrium is checked via Eq. (4).
6. If step 5 is satisfied the converged values of P, T, x_i, y_i are recorded.
7. If step 5 is not satisfied, calculations are repeated with new

assumptions from step 2.

RESULTS AND DISCUSSION

The hydrate equilibrium pressure at different initial gas CO_2 concentrations is determined and compared with the most accurate experimental data obtained from different sources [4,5,9] in Tables 1 and 2. The reported equilibrium pressure at a given initial gas CO_2 concentration is the mean average value of the three different experimental equilibrium pressures given in the above literature sources. Using the VW mixing rule, the predicted hydrate equilibrium conditions are not accurate enough at low concentration of 8% as shown in Fig. 1. However, by using the ADT mixing rule the SRK EOS give accurate predictions of hydrate equilibrium conditions as shown in Fig. 2. It seems that at lower CO_2 concentrations the polar-nonpolar interactions between H_2O and CH_4 molecules are stronger such that the VW mixing rule is not applicable.

At a high CO_2 concentration of 39%, the predicted hydrate equilibrium pressures by using the ADT mixing rule are not accurate as shown in Fig. 3. At high CO_2 concentrations the polar-nonpolar interaction between H_2O and CH_4 molecules is weaker such that the ADT mixing rule does not give good predictions. For high CO_2 concentrations the VW mixing rule is adequate for accurate prediction of hydrate equilibrium pressure as shown in Fig. 4. For all CO_2 con-

Table 1. Comparison of calculated and measured hydrate equilibrium pressures using ADT mixing rule

CO_2 mol%	T (K)	$P_{i,exp}$ (bar)	$P_{i,calc}$ (VPT)	$P_{i,calc}$ (SRK)
8%	277.8	38.3	39.1	38.9
8%	280.2	49.1	50.0	49.6
8%	283.2	68.0	69.7	68.3
8%	285.1	84.0	86.7	84.7
13%	276.9	32.4	33.1	33.0
13%	279.1	41.8	41.5	41.3
13%	281.6	53.8	54.1	53.9
13%	284.0	71.7	71.0	70.5
22%	279.4	39.6	39.79	40.93
39%	283.1	54.3	51.2	50.1
39%	285.1	69.4	66.5	64.5
39%	287.4	97.8	94.5	90.4

Table 2. Comparison of calculated and measured hydrate equilibrium pressures using VW mixing rule

CO_2 mol%	T (K)	$P_{i,exp}$ (bar)	$P_{i,calc}$ (VPT)	$P_{i,calc}$ (SRK)
8%	277.8	38.3	39.4	39.6
8%	280.2	49.1	50.5	50.8
8%	283.2	68.0	70.1	71.0
8%	285.1	84.0	87.4	88.8
13%	276.9	32.4	33.2	33.4
13%	279.1	41.8	41.6	42.1
13%	281.6	53.8	54.4	55.2
13%	284.0	71.7	71.6	73.0
22%	279.4	39.6	39.80	39.74
39%	283.1	54.3	51.0	52.4
39%	285.1	69.4	66.0	68.5
39%	287.4	97.8	92.9	100.1

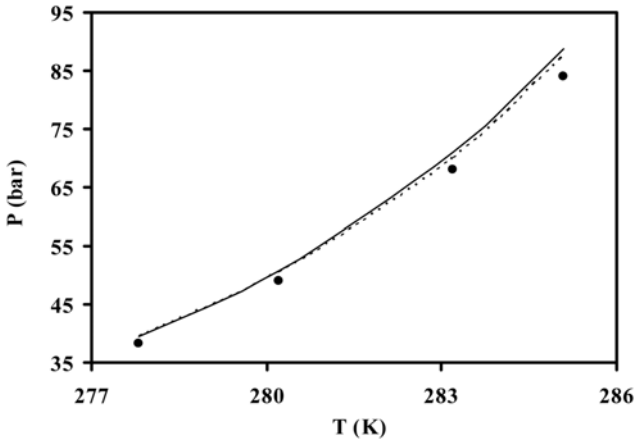

Fig. 1. Comparison between model predictions and experimental using VW mixing rule (— SRK EOS, …. VPT EOS, ● Experimental data) at CO2=8%.

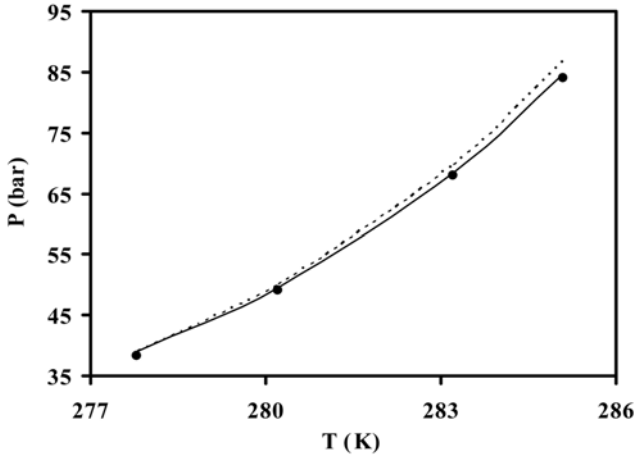

Fig. 2. Comparison between model predictions and experimental data using ADT mixing rule (— SRK EOS, …. VPT EOS, ● Experimental data) at CO2=8%.

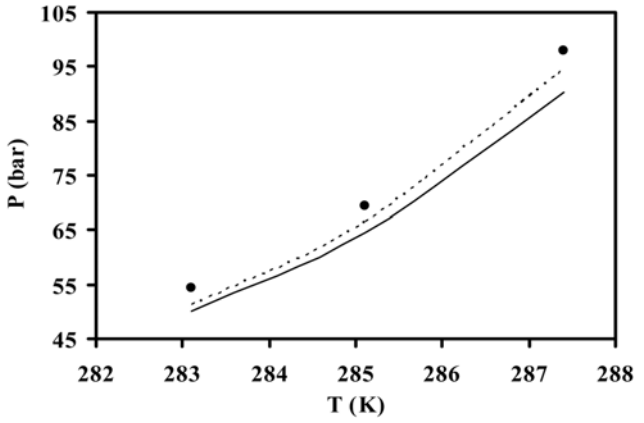

Fig. 3. Comparison between model predictions and experimental data using ADT mixing rule (— SRK EOS, …. VPT EOS, ● Experimental data) at CO2=39%.

centration ranges the predicted hydrate equilibrium pressures are usually more accurate at lower temperatures as shown in Figs. 1-4.

The average absolute deviations (AADs) in predicting the hydrate equilibrium pressures using different combinations of EOSs and mixing rules are calculated by the following equation:

$$AAD = \frac{1}{ND}\sum_{i=1}^{N}\frac{|P_{i,calc} - P_{i,exp}|}{P_{i,exp}} \quad (24)$$

where $P_{i,calc}$ and $P_{i,exp}$ are the calculated and measured hydrate equilibrium pressures respectively and ND is total number of data points. The calculated errors are plotted versus CO_2 concentrations in Fig. 5. As shown, the SRK EOS with ADT mixing rule gives the minimum error at a CO_2 molar concentration of 8%, which is in agreement with the results obtained in Fig. 2. However, at a CO_2 concentration as high as 39%, the VW mixing rule gives better predictions, which is in agreement with the results obtained in Fig. 4. Regarding hydrate equilibrium conditions in the CO_2 concentration range of 13-22%, the VPT EOS shows better performance as compared to SRK EOS as shown in Fig. 5.

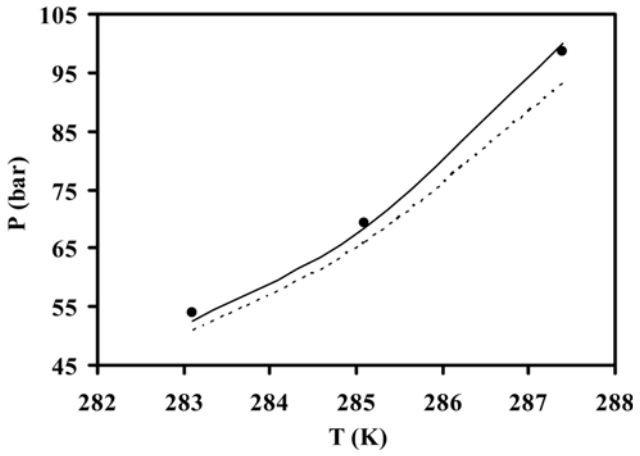

Fig. 4. Comparison between model predictions and experimental data using VW mixing rule (— SRK EOS, …. VPT EOS, ● Experimental data) at CO2=39%.

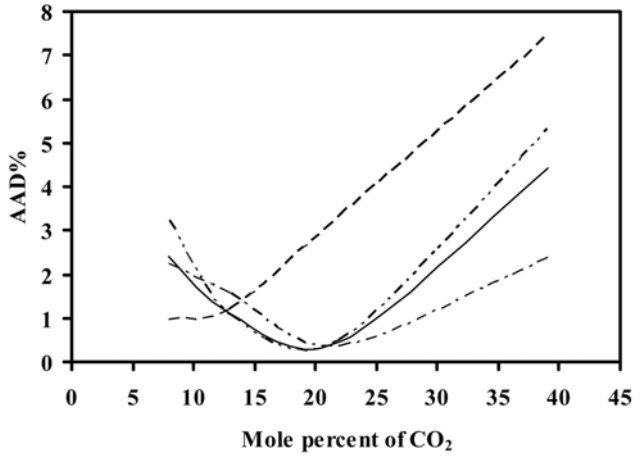

Fig. 5. AAD% between predicted and experimental data using different combinations of EOSs and mixing rules (– · – SRK+VW, — VPT+ADT, – · · – VPT+VW, – – SRK+ADT).

CONCLUSIONS

Effect of CO_2 concentration on the performance of different thermodynamic models for prediction of CH_4+CO_2+H_2O hydrate equilibrium conditions has been investigated in this work. The SRK EOS with ADT mixing rule gives the most accurate predictions at low CO_2 concentration, while the SRK EOS with VW mixing rule gives better predictions at high CO_2 concentrations. For the moderate range of CO_2 concentration (13-22%), the VPT EOS is preferred over SRK EOS, and the aforementioned mixing rules give similar results. The proposed thermodynamic approach can be used for accurate design of methane recovery processes via carbon dioxide injection into methane hydrate reservoirs.

NOMENCLATURE

$\Delta\mu_w^{H-MT}$: difference of the chemical potential of water between the hydrate phase and the empty hydrate lattice [J·mol^{-1}]
$\Delta\mu_w^{MT-L}$: difference of the chemical potential of water between the empty hydrate lattice and the liquid phase [J·mol^{-1}]
$\Delta\mu_w^{H}$: chemical potential of water in a filled hydrate lattice [J·mol^{-1}]
$\Delta\mu_w^{MT}$: chemical potential of water in an empty hydrate lattice [J·mol^{-1}]
$\Delta\mu_w^{L}$: chemical potential of water in the liquid phase [J·mol^{-1}]
$\Delta\mu_w^{0}$: water chemical potential difference at the reference condition [J·mol^{-1}]
Δh_w^{MT-L} : water enthalpy difference between the empty lattice and the liquid phase [J·mol^{-1}]
Δv_w^{MT-L} : water molar volume difference between the empty hydrate lattice and the liquid phase [m^3·mol^{-1}]
$\hat{f}_i^L$: fugacity of component i in the liquid phase [bar]
$\hat{f}_i^V$: fugacity of component i in the vapor phase [bar]
a_c : Kihara hard core parameter [m]
AAD : average absolute deviation
a,b,c : equation of state parameters
a^W : Van der Waals mixing parameter
a^A : correction term for asymmetric interaction in ADT mixing rule
C_{mj} : Langmuir constant of component j on the cavity of type m [J^{-1}m^3]
F : parameter in Eq. (17)
i, j : components i and j
k_{ij} : interaction coefficient between components of i and j
k : Boltzmann constant [J·K^{-1}]
l_{pi} : correction function between molecule of i and polar molecule of p in ADT mixing rule
l_{pi}^0, l_{pi}^1 : fitting parameters of ADT mixing rule
m_s : parameter in Eq. (12)
m : type of cavity
N : exponent number in Eq. (7)
NC : number of nonpolar components
NCA : number of cavity types
ND : number of data points
NH : number of hydrate former components
NP : number of polar components
P : pressure [bar]
P_0 : reference pressure [bar]

P_c : critical pressure [bar]
$P_{i,calc}$: calculated hydrate equilibrium pressure [bar]
$P_{i,exp}$: measured hydrate equilibrium pressure [bar]
p : index polar component
R_c : average radius of the cavity
R : universal gas constant
r : radial distance from the cavity center [m]
T : temperature [K]
T_0 : freezing point of water [K]
T_c : critical temperature [K]
T_r : reduced temperature
U, W : parameters in Eq. (8)
w(r) : spherical-core potential [J]
x_i : mole fraction of component i in the liquid phase
x_w : mole fraction of water in the water rich solution
x_p : mole fraction of polar component p
y_i : mole fraction of component i in the vapor phase
Z : coordination number
Z_c : critical compressibility factor
z_i : mole fraction of component i in the feed gas mixture
v_m : number of cavities of type m per water molecule in the hydrate lattice
v : molar volume [$m^3 \cdot mol^{-1}$]
ω : acentric factor
ε : Kihara energy parameter [J]
σ : Kihara size parameter [m]
δ : parameter in Eq. (6)
γ_w : activity coefficient of water in the water rich solution
α : SRK EOS parameter in Eq. (11)

REFERENCES

1. A. V. Milkov, *Earth Science Reviews*, **66**, 183 (2004).
2. I. Chatti, L. Delahaye, L. Fournaison and J. P Petitet, *Energy Convers. Manage.*, **46**, 1333 (2005).
3. D. A. Gunn, L. M. Nelder, C. A. Rochelle, K. Bateman, P. D. Jackson, M. A. Lovell, P. R. N. Hobbs, D. Long, J. G. Rees, P. Schultheiss, J. Roberts and T. Francis, *Terra Nova*, **14**, 43 (2002).
4. K. Ohgaki, H. Sangawa, T. Matsubara and S. Nakano, *J. Chem. Eng. Japan*, **29**, 478 (1996).
5. H. Lee, Y. Seo, I. L. Moudrakovski and A. Ripmeester, *Angew. Chem. Int. Ed.*, **42**, 5084 (2003).
6. E. M. Yezdimer, P. T. Cummings and A. A. Chialvo, *J. Phys. Chem.*, **106**, 7982 (2002).
7. T. Komai, T. Kawamura, S. Kang, K. Nagashima and Y. Yamamoto, *J. Phys. Condens Matter.*, **14**, 1395 (2002).
8. S. Hirohama, Y. Shimoyama, A. Wakabayashi, S. Tatsuta and N. Nishida, *J. Chem. Eng. Japan*, **29**, 1014 (1996).
9. E. D. Sloan and C. A. Koh, *Clathrate hydrates of natural gases*, Chemical Industries, CRC Press, 3rd Ed. (2008).
10. G. Soave, *Chem. Eng. Sci.*, **4**, 1197 (1972).
11. J. O. Valderrama, *J. Chem. Eng. Japan*, **23**, 87 (1990).
12. D. Avlonitis, A. Danesh and A. C. Todd, *Fluid Phase Equilibria*, **94**, 181 (1994).